Level structure of the $T_z = -1$ nucleus ^{34}Ar and its relevance for nucleosynthesis in ONe novae

A. R. L. Kennington,[1] G. Lotay,[1] D. T. Doherty,[1] D. Seweryniak,[2] C. Andreoiu,[3] K. Auranen,[2,*] M. P. Carpenter,[2] W. N. Catford,[1] C. M. Deibel,[4] K. Hadyńska-Klęk,[1,†] S. Hallam,[1] D. Hoff,[5] T. Huang,[2] R. V. F. Janssens,[6,7] S. Jazrawi,[1] J. José,[8,9] F. G. Kondev,[2] T. Lauritsen,[2] J. Li,[2] A. M. Rogers,[5] J. Saiz,[10] G. Savard,[2] S. Stolze,[2] G. L. Wilson,[2,4] and S. Zhu[2,‡]

[1]*Department of Physics, University of Surrey, Guildford, GU2 7XH, United Kingdom*
[2]*Physics Division, Argonne National Laboratory, Argonne, Illinois 60439, USA*
[3]*Department of Chemistry, Simon Fraser University, Burnaby, British Columbia, Canada V5A 1S6*
[4]*Department of Physics and Astronomy, Louisiana State University, Baton Rouge, Louisiana 70803, USA*
[5]*Department of Physics and Applied Physics, University of Massachusetts Lowell, Lowell, Massachusetts 01854, USA*
[6]*Department of Physics, University of North Carolina at Chapel Hill, Chapel Hill, North Carolina 27599, USA*
[7]*Triangle Universities Nuclear Laboratory, Duke University, Durham, North Carolina 27708, USA*
[8]*Departament de Física, Universitat Politècnica de Catalunya,E-08019 Barcelona, Spain*
[9]*Institut d'Estudis Espacials de Catalunya (IEEC), E-08034 Barcelona, Spain*
[10]*Department of Physics, University of York, Heslington, York, YO10 5DD, United Kingdom*

(Received 7 January 2021; accepted 10 February 2021; published 8 March 2021)

The ^{24}Mg + ^{12}C fusion reaction was used to perform a detailed γ-ray spectroscopy study of the astrophysically important nucleus ^{34}Ar. In particular, an experimental setup, coupling the advanced γ-ray tracking array GRETINA with the well-established Argonne fragment mass analyzer (FMA), was employed to obtain excitation energies and spin-parity assignments for excited states in ^{34}Ar, both above and below the proton separation energy. For the first time, an angular distribution analysis of in-beam γ rays from fusion-evaporation reactions, using a tracking array, has been performed and Coulomb energy differences of analog states in the $T = 1$, $A = 34$ mirror system, explored from 0 to 6 MeV. Furthermore, we present a comprehensive discussion of the astrophysical ^{33}Cl(p, γ) stellar reaction rate, together with implications for the identification of nova presolar grains from sulfur isotopic abundances.

DOI: 10.1103/PhysRevC.103.035805

I. INTRODUCTION

One of the most fundamental properties of the nuclear force is that it is independent of the charge of the individual nucleons between which it acts. This fascinating feature allows us to treat the interactions of protons and neutrons as indistinguishable, and leads naturally to the concept of isospin [1]. That is, nuclear states with the same isospin quantum number T, and the same total number of nucleons, may be described with the exact same wave function. Such exchange symmetries can be readily observed in the behavior of nuclei throughout the chart of nuclides. In particular, the structures of mirror nuclei (nuclei with opposite numbers of protons and neutrons) have been found to be almost identical.

In this regard, experimental studies using large HPGe detector arrays have allowed for a detailed exploration of the level structures of $T = 1/2$ mirror nuclei, from the ground state up to energies of interest for explosive hydrogen burning. Initially, investigations in the *sd* shell were strongly focused on high-spin states [2,3], while detailed experimental and theoretical studies in the region between ^{40}Ca and ^{56}Ni [4–6] were instantly possible, owing, in part, to the relative isolation of the $f_{7/2}$ shell. However, more recently, investigations of the $A = 23$ [7,8], 27 [9,10], and 31 [11,12] analog systems, using the world-leading Gammasphere array, provided some of the most comprehensive information on the evolution of mirror energy differences (MEDs) in the *sd* shell, as well as significantly reduced uncertainties in the astrophysical ^{22}Na(p, γ), ^{26}Al(p, γ), and ^{30}P(p, γ) reactions, respectively.

Extending the detailed measurement of analog nuclear states to more exotic $T = 1$ isobaric triplet systems has proven to be an experimental challenge, owing to the much reduced production cross sections. However, recent experimental advancements in the amalgamation of γ-ray tracking technology with precision recoil detection have now opened up a variety of possibilities for the investigation of $T = 1$ nuclei across the *sd* and *fp* shells [13]. Here, we report on a comprehensive study of the $T_z = -1$ nucleus ^{34}Ar, which makes use of the advanced γ-ray tracking array GRETINA [14], in conjunction with the Argonne fragment mass analyzer (FMA) [15]. In particular, we considerably expand upon an earlier Letter [16], which concentrated on proton-unbound states in ^{34}Ar that govern the rate of the ^{33}Cl(p, γ) reaction, and present, for the

*Present address: Department of Physics, University of Jyvaskyla, P.O. Box 35, FI-40014, Finland.
†Present address: Heavy Ion Laboratory, University of Warsaw, Pasteura 5a, 02-093 Warsaw, Poland.
‡Present address: Brookhaven National Laboratory, National Nuclear Data Center, Upton, New York 11973, USA.

 ©2021 American Physical Society

first time, an in-beam angular distribution analysis of γ rays, using a tracking array. Moreover, we explore the evolution of mirror energy differences in the $A = 34$ system, together with a comparison to shell-model calculations, and address the implications of the current data for the identification of nova presolar grains [17–19].

II. EXPERIMENTAL SETUP

The ATLAS facility, at Argonne National Laboratory, was used to produce an ≈15 pnA beam of ^{24}Mg ions at 95 MeV. This beam was then used to bombard an ≈200-μg/cm^2-thick ^{12}C target for a period of ≈140 h to produce ^{34}Ar, ^{34}S, and ^{34}Cl nuclei via the $2n$, $2p$, and $1p1n$ evaporation channels, respectively (the simultaneous observation of the ^{34}Ar mirror nucleus ^{34}S is of particular importance for the present work). Prompt γ rays were registered with the tracking array GRETINA [14], which, in this instance, consisted of 12 modules with four segmented HPGe detectors each, while recoils from fusion-evaporation reactions, $Q = 13^+$, (average velocity, $\beta = v/c = 0.0637$) were analyzed and separated using the fragment mass analyzer [15]. The relative positions of recoiling ions at the focal plane were determined with a position-sensitive parallel-grid avalanche counter (PGAC) and atomic number Z selectivity was achieved using an ionization chamber (IC). Here, three energy loss signals were analyzed (ΔE_1, ΔE_2, and ΔE_3). Optimum Z separation was observed by analyzing histograms where the sum of ΔE_1 and ΔE_2 signals were plotted against the total energy deposited ($\Delta E_1 + \Delta E_2 + \Delta E_3$), as shown in Fig. 1 of Ref. [16]. Energy and efficiency calibrations of GRETINA were performed using standard ^{152}Eu and ^{56}Co calibration sources, under identical tracking conditions [20] to those used in the experiment. The data acquisition was triggered when an event was registered in the focal plane detectors. The γ-ray events of interest were then selected by setting appropriate conditions on the energy loss in the IC, as discussed above. Examples of the resulting γ-ray singles spectra are shown in Fig. 1, where the top spectrum [Fig. 1(a)] is observed in coincidence with any recoil registered at the focal plane, while Figs. 1(b)–1(d) correspond to the selection of S, Cl, and Ar ions, respectively.

The x position at the FMA focal plane is a linear function of the the M/Q value of the recoil. Consequently, additional selectivity was achieved using information from the PGAC, which allowed for conditions to be set on the position, along the x axis, of the recoils. This condition proved to be effective in removing, for example, ^{37}Ar, which arises from ^{16}O(^{24}Mg, $2pn$) reactions from oxygen contamination on the targets.

Based on the observed peak areas in the recoil-gated γ-ray spectra, and accounting for relative FMA acceptances and charge-state distributions, the ^{34}Ar production cross section was estimated to be ≈10 μb. Consequently, the greater efficiency of GRETINA in the detection of high-energy γ rays, over traditional arrays (e.g., Gammasphere), together with the significant increase in solid angle acceptance for recoils, afforded by the coupling of GRETINA with the FMA (compared to the Gammasphere + FMA setup), marks a clear step change for the experimental investigation of exotic nuclei of astrophysical importance.

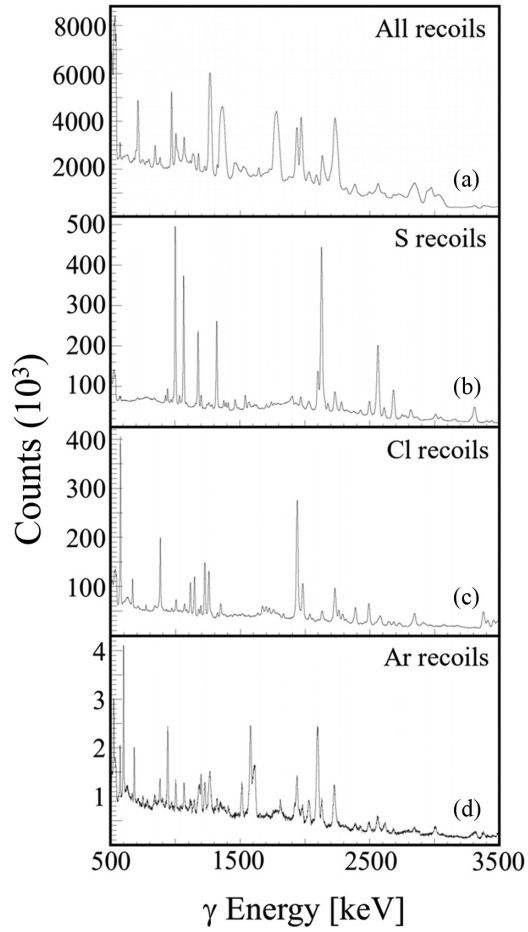

FIG. 1. Portions of the γ-ray singles spectra observed in coincidence with (a) all recoils, (b) S, (c) Cl, and (d) Ar recoils, following the application of suitable gating conditions in the ionization chamber (IC), as discussed in the text.

III. RESULTS

The level structure of ^{34}Ar was deduced by analyzing both recoil-gated γ-ray singles spectra and γ-γ coincidence matrices. An example γ-γ coincidence spectrum, with a gate placed on the 2091-keV, $2_1^+ \rightarrow 0_1^+$ transition in ^{34}Ar, is illustrated in Fig. 2, and a summary of the properties of excited states in ^{34}Ar, together with a comparison to shell-model calculations and the mirror nucleus ^{34}S, is presented in Table I. Excitation energies were determined by summing γ-ray energies following the application of a recoil correction. For states where several γ cascades were observed from the same level, a weighted average was employed to derive the excitation energy. Details of individual spin-parity assignments, incorporating both present data and previous literature, are given in Sec. IV.

An angular distribution analysis was also performed for the most intense transitions in ^{34}Ar and for corresponding mirror analogs in ^{34}S. Specifically, GRETINA data were divided into eight angular bins, where the polar angle θ relative to the beam axis was determined from the first (highest energy) interaction point of the γ ray in the array. Moreover, angles symmetric with respect to 90° in the forward and backward directions

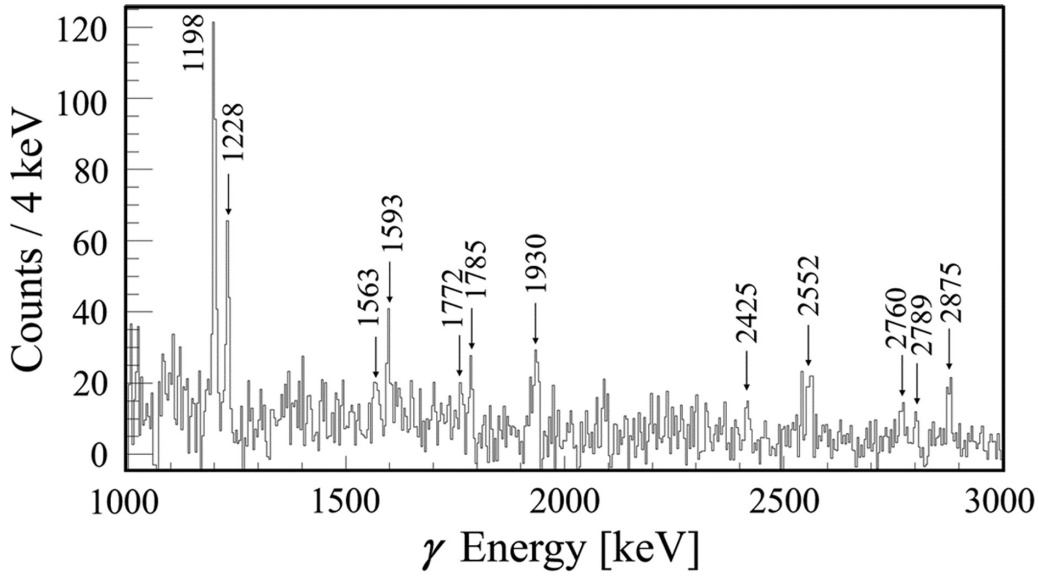

FIG. 2. A γ-ray spectrum gated on the 2091-keV, $2_1^+ \rightarrow 0_1^+$ transition in ^{34}Ar. The peaks are labeled with transition energies given in keV.

were summed because of the limited statistics available. Angular distributions were then extracted and fit as a function of angle using the function $W(\theta) = a_0\{1 + a_2P_2(\cos(\theta) + a_4P_4(\cos\theta)\}$, where P_2 and P_4 represent the Legendre polynomials and the coefficients a_2 and a_4 contain information on the multipolarity of the transition. Dipole transitions, $\Delta J = 1$, have negative a_2 values while quadrupole transitions, $\Delta J = 2$, have positive a_2 values.

Observed distributions for both $\Delta J = 1$ and $\Delta J = 2$ transitions are presented in Fig. 3. This represents, to the best of our knowledge, the first time that angular distributions of in-beam γ rays have ever been reported for a Ge array utilizing the technique of γ-ray tracking. In this regard, it should be noted that extracting angular distributions reliably with a tracking array presents a significant experimental challenge, owing to both the strong energy dependence of the array and the fact that, at present, such arrays do not offer 4π coverage and, therefore, the number of physical spaces, relative to Ge, changes as a function of polar angle θ. Consequently, the experiment and analysis reported here represent a somewhat unique case. First, the energies of the transitions examined in Fig. 3 are similar to the energies of lines in the

TABLE I. Properties of excited states in ^{34}Ar. Previous excitation energies and spin-parity assignments for states in ^{34}Ar and ^{34}S have been taken from Ref. [21]. Level energies have been corrected for the recoil of the compound nucleus. Details of shell-model (SM) calculations are given in the text.

$E_{x,^{34}\mathrm{Ar}}$ (keV) [21]	J^π [21]	$E_{x,^{34}\mathrm{Ar}}$ (keV) present	E_γ (keV)	J_n^π	$E_{x,^{34}S}$ (keV) [21]	$E_{x,\mathrm{SM}}$ (keV)
2091.1(3)	2^+	2091.4(5)	2091.3(5)	2_1^+	2128	2106
3287.7(5)	2^+	3289.0(7)	1197.5(4)	2_2^+	3304	3266
			3289.1(10)			
3873.0(30)	0^+	3876.2(9)	1784.8(8)	0_1^+	3916	3899
4050(14)		4020.8(18)	1930.4(23)	2_3^+	4115	4319
			4019.8(15)			
4127.8(10)		4131.7(10)	842.5(7)	1_1^+	4075	3694
4513.2(8)	3^-	4517.3(10)	1228.4(5)	3_1^-	4624	5424
			2424.7(22)			
4631(4)		4643.9(9)	2552.4(8)	4_1^+	4689	4808
4865(4)		4851.6(13)	1562.8(7)	3_1^+	4877	4836
			2759.9(12)			
		4881.3(21)	1592.5(17)	2_4^+	4890	4533
			2788.9(19)			
			4881.9(24)			
4967(4)	0^+	4963.8(13)	832.1(9)	0_2^+	5228	5370
		4966.7(11)	2875.2(10)	2_1^-	5323	6172
		5060.8(13)	1771.8(11)	1_2^+	5381	5602
			(5062)			

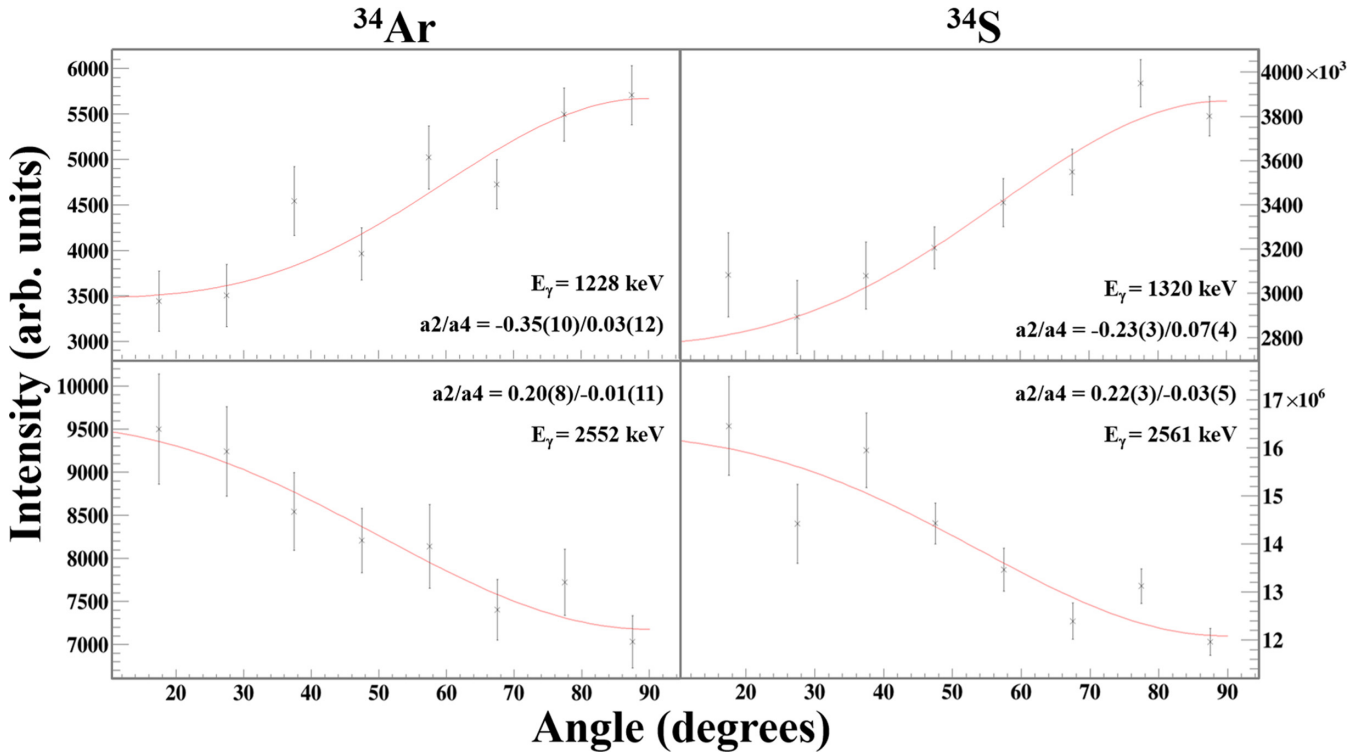

FIG. 3. Example γ-ray angular distributions obtained in the present work for both ^{34}Ar and ^{34}S. $\Delta J = 1$ transitions are shown on the top row while $\Delta J = 2$ transitions are given at the bottom. The error bars on the data points reflect the statistical uncertainty on the extracted γ-ray intensities.

^{152}Eu and ^{56}Co sources used for efficiency calibration, which limits the effect of energy dependency. Furthermore, the channel selectivity provided by the FMA significantly reduced Compton background from intense higher-energy transitions. This has a different energy response to the decays of interest and, as such, complicates the extraction of angular distributions. Finally, it should be noted that no sensitivity was observed between $\Delta J = 2$ and $\Delta J = 0$ transitions, which may have similar a_2 and a_4 values, owing to the limited statistics obtained in the present study. Thus, caution must be taken when planning to use data from experiments employing γ-ray tracking arrays to make firm spin-parity assignments (for example, as is proposed in Ref. [22]), particularly when additional information, such as the properties of levels in the mirror nucleus, is scarce.

IV. DISCUSSION

Figure 4 illustrates a proposed matching of analog levels in the $T = 1$, $A = 34$ mirror system ^{34}Ar-^{34}S, up to an excitation energy of ≈6 MeV. Also included is a comparison of experimentally observed excitation energies with the results of shell-model calculations. These calculations were performed based on a USDA Hamiltonian, within the *sd* shell-model space [23] for even-parity states, and on the WBP Hamiltonian, which includes a *sd*-*pf* model space for odd-parity levels [24]. In the sections below, the spin-parity assignments of levels in ^{34}Ar are justified in detail, drawing on both the present experimental information and previous work. In addition, the evolution of mirror-energy differences between analog states is discussed, particularly for states which deviate from the generally observed trends—in the text that follows, MED is defined as $E_x(^{34}\mathrm{S})$-$E_x(^{34}\mathrm{Ar})$.

A. Bound levels in ^{34}Ar

The properties of the 2_1^+, 2_2^+, and 0_1^+ excited states in ^{34}Ar have already been well established [21], and both the excitation energies and matching to mirror states in ^{34}S are confirmed here. However, little information was previously reported on excited states above 4 MeV in the nucleus ^{34}Ar.

1. E_x = 4021 and 4132 keV

In the present work, an excited state at 4020.8(18) keV in ^{34}Ar was found to exhibit a strong γ-decay branch to the ground state, together with an additional 1930.4(23)-keV transition to the 2_1^+ level, while a higher-lying level at 4131.7(10) keV was observed to decay solely to the 2_2^+ excited state. From an examination of the mirror nucleus ^{34}S, over the energy range $E_x = 3.5$–4.5 MeV, we find that both the 1_1^+, 4075-keV and 2_3^+, 4115-keV levels are known to γ decay to the ground and 2_1^+ states [21]. However, only the 1_1^+, 4075-keV state in ^{34}S is known to exhibit a γ-ray branch to the 2_2^+ level. This transition was also observed in the current study and, as such, we assign the present 4021-keV and 4132-keV excited states in ^{34}Ar as the 2_3^+ and 1_1^+ levels, respectively. These assignments imply a negative MED value (−57 keV) between 1_1^+ states in the $A = 34$ system, which is in contrast

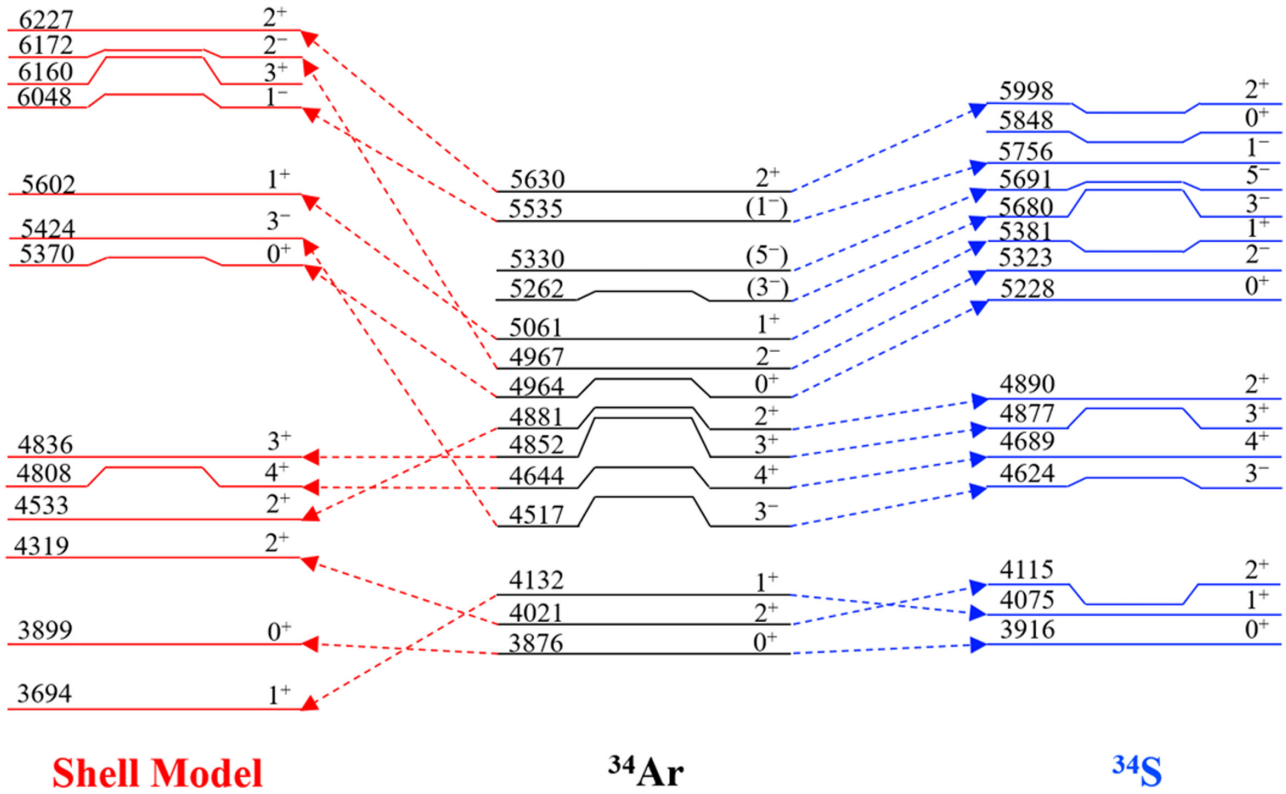

FIG. 4. Proposed assignments of analog states in the $T = 1$, ^{34}Ar-^{34}S mirror system for excitation energies up to ≈6 MeV, together with a comparison with shell-model calculations. Excitation energies for levels in ^{34}Ar above 5061 keV are taken from the ^{36}Ar(p, t) reaction study of Long *et al.* [25].

to the positive MEDs observed for most analog states (see Fig. 4). However, the magnitude of this energy difference is small and is in line with shifts observed in other nuclei in the *sd* shell [9]. Furthermore, we note that in a recent ^{36}Ar(p, t) ^{34}Ar reaction study by Long *et al.* [25], an excited state at 4019.1(43) keV was strongly observed, whereas no evidence for the population of a level at 4132 keV was reported, adding additional support for the assignments presented here.

2. $E_x = 4517$ keV

The known 3^-_1 level in ^{34}Ar is strongly populated in the current study and we report γ decays to the 2^+_1 and 2^+_2 excited states, in agreement with earlier work [21], and consistent with the decay pattern of the analog 3^-_1, 4624-keV state in ^{34}S. In addition, an angular distribution analysis of the 1228-keV γ ray, that depopulates the 4517-keV level in ^{34}Ar, reveals a_2 and a_4 coefficients consistent with a $\Delta J = \pm 1$ transition, supporting a 3^-_1 assignment. However, we note that the 4517.3(10)-keV excitation energy determined in this work is in disagreement with that reported in Ref. [21]. At present, we do not have an explanation for this observed discrepancy and thus, are restricted to simply highlighting it here.

3. $E_x = 4644$ keV

Considering Fig. 2, an intense γ-γ coincidence relationship with the $2^+_1 \rightarrow 0^+_1$ transition in ^{34}Ar is observed at 2552.4(8) keV, indicating the presence of an excited state at 4643.9(9) keV. No further decays were observed from this level and a comparison with the mirror nucleus ^{34}S, in the excitation energy region from 4.1 to 5.1 MeV, reveals that only the 4^+_1, 4689-keV state exhibits a 100% branch to the 2^+_1 level. Thus, a 4^+_1 assignment is proposed for the 4643.9(9)-keV level in ^{34}Ar. This assignment is further strengthened by an angular distribution analysis of the 2552-keV γ ray that depopulates the state, which produces a_2 and a_4 coefficients that are consistent with a $\Delta J = \pm 2$ transition.

B. Proton-unbound levels in ^{34}Ar

In total, γ rays from five excited states above the proton-emission threshold of $S_p = 4663.9(4)$ keV [26] in ^{34}Ar are observed in the present work.

1. $E_x = 4852$ and 4881 keV

Here, the lowest-lying proton-unbound excited state in ^{34}Ar is found to appear at 4851.6(13) keV. This level, which was previously observed at 4865(4) keV [21], de-excites via both a 2759.9(12)-keV γ ray directly to the 2^+_1 level, as shown in Fig. 2, and a weaker 1562.8(7)-keV transition to the 2^+_2 state. Intriguingly, similar decay branches, to the first two 2^+ states, are observed for a nearby 4881.3(21)-keV excited state in ^{34}Ar. However, for the 4881-keV level, whose excitation energy is in good agreement with an earlier reported value [25], an additional 4881.9(24)-keV transition direct to the ground state is also observed. An examination of the mirror

nucleus ^{34}S in the excitation energy region 4.7–5.3 MeV, indicates that only the 3_1^+, 4877-keV state and 2_4^+ level at 4890 keV exhibit decay branches to the 2_1^+ and 2_2^+ excited states. A direct to ground-state transition would not be observed for a 3^+ level and, as such, a spin parity of 3^+ is ruled out for the presently observed 4881-keV level. Thus, we assign the 4852- and 4881-keV excited states in ^{34}Ar as 3_1^+ and 2_4^+, respectively.

2. $E_x = 4964$ keV

Only a single, low-energy decay branch, to the 1_1^+ level, is observed from an excited state in ^{34}Ar at 4963.8(13) keV. The derived excitation energy in the present study is in reasonable agreement with the established 0_3^+ level in ^{34}Ar, populated in the ^{36}Ar(p, t) reaction [25]. Furthermore, this characteristic de-excitation path is only observed from the known analog 0_3^+, 5228-keV state in ^{34}S, over the energy range $E_x = 4.5 - 5.8$ MeV. Consequently, a 0_3^+ assignment is proposed for the presently observed 4964-keV level in ^{34}Ar.

3. $E_x = 4967$ keV

An inspection of Fig. 2 reveals the presence of a high-intensity coincidence relationship at 2875.2(10) keV, leading to an excited state in ^{34}Ar at 4966.7(11) keV. This level cannot be the same as the 0_3^+ level described above based on the different excitation energy. Moreover, an angular distribution analysis of the 2875-keV γ ray results in a_2 and a_4 values of 0.9(3) and 0.4(5), respectively, consistent with a $\Delta J = 0$ transition. We note that the experimental uncertainties are large. However, the observation of a positive, nonzero a_2 coefficient rules out a 0^+ assignment and points toward a spin of $J = 2$ for the 4967-keV state. In this regard, the 2_1^-, 5323-keV state in the mirror nucleus ^{34}S displays a similar, single dominant de-excitation path to the 2_1^+ level. Consequently, we propose a 2_1^- level in ^{34}Ar at 4967 keV.

4. $E_x = 5061$ keV

Finally, by analyzing γ-γ coincidence relationships with the 2_2^+ level (see Fig. 4 of Ref [16]), an excited state in ^{34}Ar was established at 5060.8(13) keV. Here, the previously reported 1771.8(11)-keV transition to the 2_2^+ state, also shown in Fig. 2, provides the strongest evidence for the 5061-keV level. However, an additional, tentative, direct to ground-state 5062-keV transition was also observed. Examining the relevant energy region in the mirror nucleus ($E_x = 4.9$–5.7 MeV), indicates that only the 1_2^+ and 3_2^- levels, with respective excitation energies of 5381 and 5680 keV in ^{34}S decay to the 2_2^+ excited state. The tentative observation of direct transition to the ground state is not compatible with a 3^- spin-parity assignment (an $E3$ transition would not be observed). Furthermore, the smaller MED of ≈320 keV, rather than ≈620 keV, together with the nonobservation of a level at 5061 keV in ^{36}Ar(p, t) reaction studies [25], supports a 1_2^+ assignment. As such, we assign the presently observed 5061-keV state in ^{34}Ar as 1_2^+.

C. Higher-lying (unobserved) states

As illustrated in Fig. 4, and to further strengthen the arguments for proposed mirror matchings for the key proton-unbound levels, discussed previously, an analysis of higher-lying levels reported in previous literature was also undertaken. Excited states at 5262(16), 5330(17), 5535(18), and 5629.6(45) keV were reported in a (p, t) study of Long *et al.* [25]. Of these, the 5630-keV level was previously assigned as 2^+ [21] and a tentative $L = 5$ transfer was reported in a ^{32}S(^{3}He, n) study by Alford *et al.* [27] for the 5330-keV level, indicating a possible 5^- assignment. The 5330- and 5630-keV states in ^{34}Ar are well matched to mirror 5_1^-, 5691-keV and 2_5^+, 5998-keV analogs in ^{34}S. As such, and based on observed MEDs, we propose that the remaining, unassigned 5262- and 5535-keV levels in ^{34}Ar correspond to the 3_2^- and 1_1^- excited states, respectively.

D. Mirror energy differences and shell-model calculations

Mirror energy differences (MEDs) in the $T = 1$, $A = 34$ mirror system are observed to range from −57 to +418 keV, and, in general, increase with increasing excitation energy, as shown in Fig. 4. In terms of even-parity levels, the most striking MEDs are observed for the 1_2^+ and 2_5^+ mirror pairs. This is perhaps not so surprising, as the 1_2^+, 5061-keV and 2_5^+, 5630-keV excited levels in ^{34}Ar correspond to s-wave resonances in the ^{33}Cl $+p$ system. In general, larger MEDs are observed for odd-parity states. However, these are harder to predict and do not appear to be significantly influenced by the spin quantum number of the analog states. These observations are in good agreement with those made for other sd-shell nuclei, where the level scheme was explored from the ground state up to the excitation-energy region relevant for explosive hydrogen burning, e.g., Refs. [9–12].

Of potentially greater interest are the discrepancies between the nuclear shell model and experiment for the $T = 1$, $A = 34$ mirror system. Shell-model partners could be assigned with confidence by considering the characteristic γ-decay branches, however, significant discrepancies are observed between predicted and observed excitation energies in ^{34}Ar and ^{34}S. Such discrepancies were not observed in previous work on $T = 1/2$ mirror systems in the sd shell [9–12]. Examining Fig. 4, it is clear that the largest differences between the experimentally determined excitation energies and the results of shell-model calculations are for negative-parity states. This highlights the difficulty in performing reliable calculations for these levels, owing to the large model spaces required, and reinforces the need for experimental data up to high excitation energy.

In addition, it should be noted that the 3_2^+ shell-model state appears to be missing in the $A = 34$ mirror pair (see Fig. 4). This could be of interest for nuclear astrophysics, as the 3_2^+ level in ^{34}Ar would correspond to an additional resonance in the ^{33}Cl(p, γ) reaction. That being said, a very large energy shift from shell-model calculations would be required to place the 3_2^+ level inside the Gamow energy window of hydrogen burning for the ^{33}Cl(p, γ) reaction, and a d-wave resonance is unlikely to strongly impact the stellar reaction rate.

TABLE II. Summary of the properties of resonances in the astrophysical ^{33}Cl(p,γ) reaction. Spectroscopic factors have been adopted from Ref. [33] and γ-ray partial widths estimated from measured lifetimes in the mirror nucleus ^{34}S, unless otherwise noted. Both 1^+ and 3^- assignments are considered for the 397-keV resonance.

E_x (keV)	E_r (keV)	J^π	ℓ_p	C^2S	Γ_p (eV)	Γ_γ (eV)	$\omega\gamma$ (eV)
4643.9(9)	–	4^+	2	–	–	–	–
4851.6(13)	187.7(14)	3^+	2	0.04 [a]	6.4×10^{-10}	1.1×10^{-2}	5.6×10^{-10}
4881.3(21)	217.4(21)	2^+	0	0.02	3.2×10^{-7}	1.6×10^{-2}	2.0×10^{-7}
4963.8(13)	299.9(14)	0^+	2	0.003 [b]	1.5×10^{-7}	6.1×10^{-3} [b]	1.8×10^{-8}
4966.7(11)	302.8(12)	2^-	1	0.006	8.5×10^{-6}	2.7×10^{-2}	5.3×10^{-6}
5060.8(13)	396.9(13)	1^+	0	0.07	1.4×10^{-2}	9.3×10^{-2} [b]	4.5×10^{-3}
		3^-	1	0.17	1.1×10^{-2}	1.0×10^{-2} [b]	4.7×10^{-3}

[a]Based on the observed cross section in Ref. [33].
[b]Adopted from shell-model calculations.

V. ASTROPHYSICAL IMPLICATIONS

The properties of proton-unbound levels in ^{34}Ar [$S_p = 4663.9(4)$ keV] are expected to govern the rate of the ^{33}Cl(p,γ) reaction. This reaction is particularly important for nova explosions, which achieve peak temperatures, $T_{\rm peak}$, of 0.1–0.4 GK and enrich the interstellar medium with elements up to the Si-Ca mass region [28,29]. Fascinatingly, classical novae represent the only type of stellar explosion for which the nuclear physics input is almost entirely known with the required precision. However, uncertainties in several key reactions that influence the pathway of nucleosynthesis, in such scenarios, still remain. Consequently, it is essential that uncertainties be constrained to make precision comparisons of models of novae nucleosynthesis with the latest observational data.

In this regard, the accurate classification of presolar grains, from nova events involving massive underlying white dwarfs, is currently hindered by the unconstrained abundances of silicon and sulfur isotopes ejected during explosive events [30,31]. Specifically, previous uncertainties in the astrophysical ^{33}Cl(p,γ) reaction have been reported to lead to variations in ^{33}S abundances in classical novae by a factor of about $\approx$18 [32].

A. Previous estimates of the ^{33}Cl(p,γ) reaction

Until now, very little experimental information was available for estimates of the ^{33}Cl(p,γ) stellar reaction rate. As such, previous evaluations, used in theoretical models of novae nucleosynthesis, have been based on Hauser-Feshbach (HF) calculations. Given the inappropriateness of such calculations, for cases in which only a few resonances play a significant role, a study into the effect of nuclear reaction rate uncertainties on final nova yields by Iliadis *et al.* assigned a relatively conservative 10^4 uncertainty to the ^{33}Cl(p,γ) reaction [32].

However, to critically assess the impact of the current work, we have attempted to formulate a more realistic estimate of previous reaction rate uncertainties, based on the then known experimental information [21]. Considering Table I and Refs. [21,25], only three excited states ($E_x = 4865$, 4967, and 5262 keV) were previously known to exist above the proton-emission threshold in ^{34}Ar, within the Gamow energy window of classical novae. Consequently, to ascertain a "previous" high rate, we have assumed assignments of 2^+_4, 1^+_2, and 3^-_2 for the known 4865-, 4967-, and 5262-keV excited states in ^{34}Ar [21,25], respectively. Conversely, we have assumed assignments of 3^+_1, 0^+_2, and 5^-_1 for the "previous" low rate.

B. Present evaluation of the ^{33}Cl(p,γ) reaction

A summary of the resonant properties used for the present evaluation of the astrophysical ^{33}Cl(p,γ) reaction is given in Table II, while Fig. 5 illustrates the presently determined uncertainty in the rate over the temperature range 0.1–0.8 GK, in comparison with earlier estimates. Resonance energies and spin-parity assignments have been taken from the present work. However, resonance strengths are estimated using spectroscopic factors C^2S of mirror states, populated in the ^{33}S(d,p) transfer reaction [33], and known lifetimes of levels in ^{34}S [21]. We find that the rate is almost entirely dominated by the 397-keV resonance, except for $T < 0.2$ GK, where the $\ell = 0$ resonance at 217 keV governs the reaction. In fact, we note that if the spin-parity assignment of the 397-keV resonance was 3^-, instead of 1^+, its influence on the astrophysical ^{33}Cl(p,γ) reaction rate would, effectively, be identical. Further constraints on the rate would

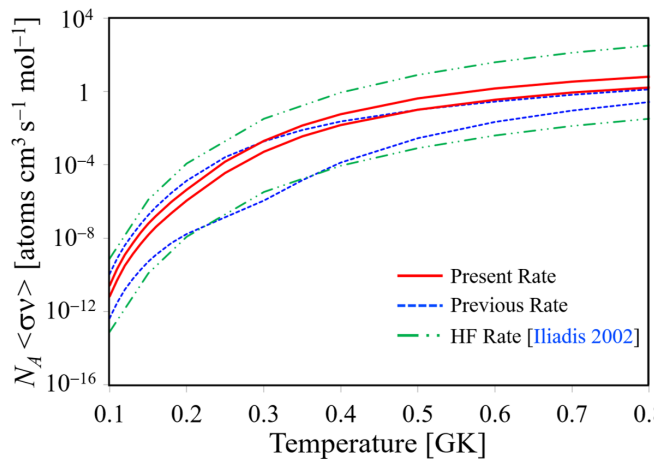

FIG. 5. Uncertainties in the ^{33}Cl(p,γ) stellar reaction rate based on the present data, in comparison with previous estimates. See text for details [32].

now require either a direct measurement of the strengths of the 217- and 397-keV resonances, or an experimental determination of their associated proton partial widths.

C. The search for nova presolar grains

To assess the implications of the present work on ejected sulfur abundances from nova events, we performed a series of simulations using the hydrodynamic, Lagrangian, time-implicit code SHIVA [34,35]. This code, which relies on a standard set of differential equations of stellar evolution in finite-difference form, was extensively used for simulations of nova outbursts, type-I x-ray bursts, and sub-Chandrasekhar supernova explosions. The equation of state used in SHIVA includes contributions from the degenerate electron gas, the ion plasma, and radiation. Coulomb corrections to the electron pressure are taken into account and radiative and conductive opacities are considered in the energy transport. Energy generation by nuclear reactions is obtained using a network that contains 120 nuclear species (from ^{1}H to ^{48}Ti), linked through 630 nuclear processes, with updated reaction rates from the STARLIB database [36]. As nucleosynthesis in the Si-Ca mass region only occurs for very massive white dwarfs, we have considered an accreting $1.35M_{\odot}$ white dwarf, with characteristic values for its initial luminosity ($10^{-2}L_{\odot}$) and mass-accretion rate ($2 \times 10^{-10}M_{\odot}$ per year). The accreted matter is assumed to mix with material from the outer layers of the white dwarf to a level of 50%. All the hydrodynamic simulations performed in this work resulted in the ejection of $\approx 5 \times 10^{-6}M_{\odot}$ of nuclear-processed material, after achieving a peak temperature of $\approx 3.1 \times 10^{8}$ K.

Focusing on ^{33}S/^{32}S isotopic ratios, our present calculations indicate that a value of ≈0.012–0.015 is to be expected in the ejecta of classical nova explosions. This is in contrast to the terrestrial value of 0.0079, as well as that predicted for type-II supernovae (0.0050–0.0077) [37]. For a comparison of the presently expected sulfur isotopic abundances in the ejecta of classical novae with recently analyzed presolar grains, we convert our predicted ^{33}S/^{32}S isotopic ratios into deviations (δ) from normal isotopic ratios in parts per thousand, using the formalism,

$$\delta\,^{33}\mathrm{S}/^{32}\mathrm{S} = \left[\frac{(^{33}\mathrm{S}/^{32}\mathrm{S})_{\mathrm{grain}}}{(^{33}\mathrm{S}/^{32}\mathrm{S})_{\mathrm{standard}}} - 1\right] \times 1000. \qquad (1)$$

Furthermore, we adopt the experimentally constrained $\delta\,^{34}$S/^{32}S range reported in Ref. [38], based on an investigation of the ^{34}S(p,γ) reaction in classical novae environments.

Figure 6 displays the present, experimentally constrained sulfur isotopic ratios expected in the ejecta of classical novae, in comparison with extracted values from known presolar grains. It is clear, from Fig. 6, that the expected abundances of sulfur isotopes produced in nova explosions are distinctive from type-II supernovae. However, the vast majority of potential nova grains appear to be ruled out by the current findings. Nevertheless, the grain Ag2_6 exhibits $\delta\,^{33}$S/^{32}S and $\delta\,^{34}$S/^{32}S ratios that are broadly consistent with the values determined from the present SHIVA simulations. As

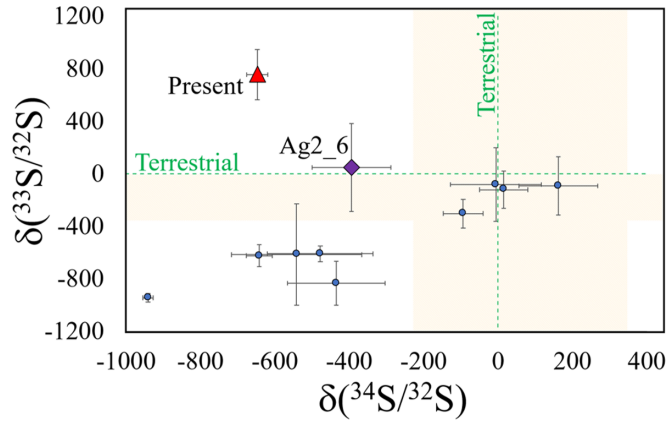

FIG. 6. Expected $\delta\,^{33}$S/^{32}S and $\delta\,^{34}$S/^{32}S ratios from the present data in comparison with extracted values from isolated presolar grains. The most promising nova grain candidate, Ag2_6 [39], is highlighted by a purple diamond, while blue circles represent data obtained on the grains: M7-C [40], M7-D [40], KJE-al-5-7 [18], G270_2 [39], GAB [39], Ag2 [39], M1-A8-G145 [41], KJD-1-11-5 [42], and KJD-3-23-5 [42]. Finally, the shaded region represents the $\delta\,^{33}$S/^{32}S and $\delta\,^{34}$S/^{32}S ratio ranges of type-II supernovae [37].

such, we propose that Ag2_6 represents the most promising candidate presolar grain for being of nova origins, based on the observed $\delta\,^{33}$S/^{32}S and $\delta\,^{34}$S/^{32}S ratios. This grain was also identified as having one of the highest probabilities of a nova paternity in Ref. [43], in agreement with the present results. However, the experimentally unconstrained, astrophysical ^{34}Cl$(p,\gamma)^{35}$Ar reaction could significantly influence the presently predicted $\delta\,^{34}$S/^{32}S ratio and, thereby, help define the origins of Ag2_6. Consequently, experimental investigations of the ^{34}Cl$(p,\gamma)^{35}$Ar reaction should be carried out as a matter of urgency.

VI. CONCLUSIONS

We have performed a detailed γ-ray spectroscopy study of the $T_z = -1$ nucleus ^{34}Ar. In particular, spin-parity assignments, together with proposed mirror matchings, have been made for all excited states in ^{34}Ar from $E_x = 0$–5.630 MeV. In comparison with the most recent structure evaluation of ^{34}Ar [21], the excitation energies of states have been measured with greater precision and spin-parity assignments have been made for all states. A comparison with shell-model calculations performed with a USDA Hamiltonian, within the *sd* shell-model space, for even-parity states, and with the WBP Hamiltonian, with an *sd-pf* space, for odd-parity levels is made. Assignments could be made with confidence based on the characteristic γ-decay branches. We note, however, that for some odd-parity levels significant deviations are observed between the experimentally measured excitation energies and those from the calculations, highlighting the need for good-quality experimental data up to high excitation energy. These findings are further supported by, to our knowledge, the first angular distribution analysis of in-beam γ rays using a tracking array, following a fusion-evaporation reaction. The resulting angular distributions were found to

be in agreement with expectations but we highlight that this experiment remains a somewhat special case because of the channel selectivity offered by the FMA.

As reported in our earlier Letter [16], the 397-keV resonance is found to dominate the ^{33}Cl$(p,\gamma)^{34}$Ar stellar reaction rate over the peak temperature range of classical nova explosions, while the $l = 0$ resonance at 217 keV governs the reaction rate for $T < 0.2$ GK. Nova outburst simulations were performed using the hydrodynamic, Lagrangian, time-implicit code SHIVA. These indicate that the presolar grain Ag2_6 represents the most promising candidate for being of nova origin, based on the observed $\delta\,^{33}$S/^{32}S and $\delta\,^{34}$S/^{32}S ratios. Additional experimental investigations of the ^{34}Cl$(p,\gamma)^{35}$Ar reaction are now strongly encouraged to further constrain the $\delta\,^{34}$S/^{32}S ratio.

ACKNOWLEDGMENTS

This work was supported by the U. S. Department of Energy, Office of Science, Office of Nuclear Physics, under Contract No. DEAC02-06CH11357 and Grants No. DEFG02-94-ER40834, No. DEFG02-97-ER41041, No. DEFG02-97-ER41043, No. DEFG02-94-ER40848, and No. DE-SC0014231. United Kingdom personnel were supported by the Science and Technologies Facilities Council (STFC) and C.A. was supported by the Natural Sciences and Engineering Research Council of Canada. J.J. acknowledges support from Spanish MINECO Grant No. AYA2017-86274-P, the E.U. FEDER funds, and AGAUR/Generalitat de Catalunya Grant No. SGR-661/2017. This research uses resources of ANL's ATLAS facility, which is a DOE Office of Science User facility.

[1] D. D. Warner, M. A. Bentley, and P. V. Isacker, Nature Phys. **2**, 311 (2006).
[2] D. G. Jenkins *et al.*, Phys. Rev. C **72**, 031303(R) (2005).
[3] J. Ekman *et al.*, Phys. Rev. Lett. **92**, 132502 (2004).
[4] S. M. Lenzi *et al.*, Phys. Rev. Lett. **87**, 122501 (2001).
[5] P. E. Garrett *et al.*, Phys. Rev. Lett. **87**, 132502 (2001).
[6] P. E. Garrett *et al.*, Phys. Rev. C **75**, 014307 (2007).
[7] D. G. Jenkins *et al.*, Phys. Rev. C **87**, 064301 (2013).
[8] D. G. Jenkins *et al.*, Phys. Rev. Lett. **92**, 031101 (2004).
[9] G. Lotay, P. J. Woods, D. Seweryniak, M. P. Carpenter, H. M. David, R. V. F. Janssens, and S. Zhu, Phys. Rev. C **84**, 035802 (2011).
[10] G. Lotay, P. J. Woods, D. Seweryniak, M. P. Carpenter, R. V. F. Janssens, and S. Zhu, Phys. Rev. Lett. **102**, 162502 (2009).
[11] D. T. Doherty *et al.*, Phys. Rev. C **89**, 045804 (2014).
[12] D. T. Doherty *et al.*, Phys. Rev. Lett. **108**, 262502 (2012).
[13] C. Langer *et al.*, Phys. Rev. Lett. **113**, 032502 (2014).
[14] S. Paschalis *et al.*, Nucl. Instrum. Methods Phys. Res., Sect. A **709**, 44 (2013).
[15] C. N. Davids and J. D. Larson, Nucl. Instrum. Methods Phys. Res., Sect. B **40–41**, 1224 (1989).
[16] A. R. L. Kennington *et al.*, Phys. Rev. Lett. **124**, 252702 (2020).
[17] S. Amari, X. Gao, L. R. Nittler, E. Zinner, J. Jose, M. Hernanz, and R. S. Lewis, Astrophys. J. **551**, 1065 (2001).
[18] Y. Xu, E. Zinner, R. Gallino, A. Heger, M. Pignatari, and Y. Lin, Astrophys. J. **799**, 156 (2015).
[19] M. Bose and S. Starrfield, Astrophys. J. **873**, 14 (2019).
[20] T. Lauritsen *et al.*, Nucl. Instrum. Methods Phys. Res., Sect. A **836**, 46 (2016).
[21] N. Nica and B. Singh, Nucl. Data Sheets **113**, 1563 (2012).
[22] W. Korten *et al.*, Eur. Phys. J. A **56**, 137 (2020).
[23] B. A. Brown and W. A. Richter, Phys. Rev. C **74**, 034315 (2006).
[24] E. K. Warburton and B. A. Brown, Phys. Rev. C **46**, 923 (1992).
[25] A. M. Long *et al.*, Phys. Rev. C **97**, 054613 (2018).
[26] M. Wang, G. Audi, A. H. Wapstra, F. G. Kondev, M. MacCormick, X. Xu, and B. Pfeiffer, Chin. Phys. C **36**, 1603 (2012).
[27] W. Alford, P. Craig, D. Lind, R. Raymond, J. Ullman, C. Zafiratos, and B. Wildenthal, Nucl. Phys. A **457**, 317 (1986).
[28] J. José, M. Hernanz, and C. Iliadis, Nucl. Phys. A **777**, 550 (2006).
[29] S. Starrfield *et al.*, Astrophys. J. **692**, 1532 (2009).
[30] J. José, M. Hernanz, S. Amari, K. Lodders, and E. Zinner, Astrophys. J. **612**, 414 (2004).
[31] A. Parikh *et al.*, Phys. Lett. B **737**, 314 (2014).
[32] C. Iliadis *et al.*, Astrophys. J. Suppl. Ser. **142**, 105 (2002).
[33] J. G. Van Der Baan and B. R. Sikora, Nucl. Phys. A **173**, 456 (1971).
[34] J. José and M. Hernanz, Astrophys. J. **494**, 680 (1998).
[35] J. José, *Stellar Explosions: Hydrodynamic and Nucleosynthesis* (CRC Press, Boca Raton, 2015).
[36] A. L. Sallaska *et al.*, Astrophys. J. Suppl. **207**, 18 (2013).
[37] A. Chieffi and M. Limongi, Astrophys. J. **764**, 21 (2013).
[38] S. Gillespie *et al.*, Phys. Rev. C **96**, 025801 (2017).
[39] N. Liu *et al.*, Astrophys. J. **820**, 140 (2016).
[40] P. Hoppe, W. Fujiya, and E. Zinner, Astrophys. J. Lett. **745**, L26 (2012).
[41] N. Liu *et al.*, Astrophys. J. Lett. **842**, L1 (2017).
[42] P. Hoppe, M. Pignatari, J. Kadolányi, E. Gröner, and S. Amari, Geochim. Cos. Act. **221**, 182 (2018).
[43] C. Iliadis *et al.*, Astrophys. J. **855**, 76 (2018).